Design of Precision Hot Embossing Machine for Micropatterning on PMMA

Sridhar P.
Department of Mechanical Engineering,
Indian Institute of Technology Delhi,
New Delhi 110016, India
e-mail: sridharpalani1993@gmail.com

Supreet S. Bahga
Department of Mechanical Engineering,
Indian Institute of Technology Delhi,
New Delhi 110016, India
e-mail: bahga@mech.iitd.ac.in

Jitendra P. Khatait[1]
Department of Mechanical Engineering,
Indian Institute of Technology Delhi,
New Delhi 110016, India
e-mail: jpkhatait@mech.iitd.ac.in

A microfluidic chip requires microchannels to be created on a substrate. This paper focuses on the design and development of a precision hot embossing machine for replication of microstructures on a polymethyl methacrylate (PMMA) substrate. Kinematic coupling using three spherical balls in radial v-grooves is used to achieve precise positioning of the mold insert with the base. Flexure-based parallel guidance mechanism is used for one degree-of-freedom (DOF) motion required for the embossing process. The mechanism allows the motion of the mold normal to the substrate surface. Flexure-based kinematic coupling with the thermal center is designed to mitigate thermal stress build-up during heating and cooling of the mold insert. An Arduino-based microcontroller is developed to control the temperature profile during the process. A prototype is fabricated and experiments are performed with an aluminum mold insert on a PMMA substrate. The result shows the feasibility of the concept and the setup can be used to develop a cost-effective precision hot embossing machine for creating micropatterns for microfluidic applications. [DOI: 10.1115/1.4051770]

1 Introduction

Microfluidics integrates operations that are performed in a whole laboratory into a simple microsized microfluidic chip. A microfluidic chip is a set of microchannels created on a material substrate. The microchannels are connected in order to achieve the desired features such as mixing, pumping, sorting, or controlling the biochemical environment. Microfluidic systems are widely used in procedures such as capillary electrophoresis, isoelectric focusing, immunoassays, flow cytometry, sample injection in mass spectrometry, polymerase chain reaction amplification, DNA analysis, separation and manipulation of cells, and cell patterning. They have great applications in the medical and pharmaceutical industries.

Different materials are used for making microfluidic chips. Each material inherently corresponds with specific microfabrication strategies and certain native properties of the device. Ren et al. compare different materials with respect to the applications and cost of production, reusability of the device, and disposable device use [1]. Thermoplastic is a good choice for making low-cost devices and can cater to a wide range of applications. Generally, for high volume production of microfluidic chips, hot embossing and injection molding are used. Micromilling and laser machining are preferred for low volume production [2]. The hot embossing process needs simpler and less expensive equipment due to the lower temperature and pressure requirements than injection molding which results in a low cost of production.

Several researchers have developed a hot embossing setup to achieve replication of micropatterns on polymethyl methacrylate (PMMA) substrate. Cogun et al. investigated the effects of embossing temperature, time, and force on the production of a microfluidic device using a PMMA substrate. The process parameters were changed to observe the variation of replication rate in width and depth as well as the symmetry of the replicated microfluidic channels. The hot embossing setup included a hydraulic press of 100 kN loading capacity, and two electric resistance heaters, each with 300 W heating capacity [3].

He et al. developed a low-pressure hot embossing setup for fabricating microlinear arrays. The setup had guiding columns, a pressure plate, a lever system, and an oven for heating [4]. The pressure was applied using weights and lever system. The setup was kept inside oven for heating which was then air cooled. Juang et al. used a setup for micro-embossing consisting of a pneumatic cylinder pump and guideways with cartridge heating and air/water cooling. The pneumatic cylinder pump provided a constant compression force during the embossing process. Cartridge heaters were used to heat the mold insert and the polymer substrate with air or water used to cool the system. Temperature profiles were obtained by placing thermocouples in the mold insert and polymer substrate [5].

Wang et al. developed an automatic fabrication system for plastic microfluidic chips. The hot embossing system used a mechanical ball bearing screw jack to apply pressure. Heating and cooling were achieved using thermoelectric modules. Hot-embossing machines, automatic aligning equipment, and thermal bonding machine were developed and integrated according to the processing techniques for plastic chip fabrication. Auxiliary functions, such as automatic de-embossing and prejoining procedures, were also realized for automatic operation [6].

However, these systems were developed to study the embossing process optimization. The design of the setup with respect to positioning accuracy, alignment, and effect of heating on thermal stress build-up is not discussed. Moreover, these systems were expensive and bulky.

In this paper, we presented the design of a precision hot embossing machine for producing micropatterns at a lower cost. The setup was developed using kinematic design principles to achieve better alignment and positioning of the tools with respect to the substrate. Heating and cooling of the tools lead to thermal stresses; therefore, the concept of the thermal center has been used to design the thermal module.

The structure of the paper is as follows: Sec. 2 discusses the hot embossing process with respect to material, embossing force, temperature, and time. The design objective and requirements are deliberated in Sec. 3. The conceptual design of the setup and different modules are discussed in Sec. 4. Construction details of different modules, design calculation, and analysis are covered in

[1]Corresponding author.

Contributed by the Manufacturing Engineering Division of ASME for publication in the Journal of Micro- and Nano-Manufacturing. Manuscript received December 23, 2020; final manuscript received July 9, 2021; published online August 13, 2021. Assoc. Editor: Massimiliano Annoni.

Sec. 5. Details of the temperature control module and proportional–integral–derivative (PID) controller are covered in Sec. 6. Experimental results and conclusion are discussed in Secs. 7 and 8, respectively.

2 Hot Embossing

Hot embossing is a process in which a master, or stamp, uses mechanical pressure and heat to plastically deform a substrate material [2]. Thermoplastic material is prepared and a patterned master is mated against it with heat and pressure to emboss features by plastic deformation.

The hot embossing process involves several steps. First, the temperature of the PMMA substrate is increased above the glass transition temperature T_g, the temperature at which the polymer changes from hard, glassy material to a soft, rubbery material. Above this temperature, the polymer becomes easy to mold. The final temperature reached is called the embossing temperature. Once the embossing temperature is reached, force is applied to the substrate. The force is increased until it reaches the maximum force called the embossing Force. The embossing force is maintained for a certain period of time called the embossing time. During this period, the polymer flows and fills all the cavities in the mold. Thereafter, the temperature is reduced to demolding temperature. During this period, the force is kept constant. After the demolding temperature is reached, and as the temperature is further reduced to ambient temperature, the force is also released. This is called demolding. The PMMA substrate is then released. The three most important process parameters that significantly affect the replication accuracy are embossing force, temperature, and time.

Different works have reported the optimum embossing parameters (embossing force, temperature, and time) for the best replication accuracy [3,4,7–9]. In all the works, a set of experiments with various combinations of the parameters were conducted. The embossed channel dimensions were compared with that of the master, and optimum parameters for the best results were reported. Li et al. have used embossing pressure of 3.2 MPa, embossing temperature of 125 °C, and embossing time of 240 s to achieve replication accuracy of 99% [9]. We have used the same parameters in this study for design calculation and analysis of various modules of the proposed setup.

3 Design Objective

The objective of this research work was to design and develop a precision hot-embossing machine for replication of microstructures from the master mold to the substrate. Design requirements were specified to achieve a good quality of replication. Precision requirements in terms of location and alignment of the tools were specified. Heating and cooling of the tools lead to thermal expansion and contraction. The design should allow an internal degree-of-freedom (DOF) to avoid the build-up of thermal stresses in the tool.

3.1 Design Requirements. Design requirements are identified and various design parameters are calculated based on the embossing process requirement. Mold insert and substrate materials are selected. The process leads to design requirements for the setup in terms of positioning and alignments.

3.1.1 Substrate Material PMMA. Polymethyl methacrylate is selected as a substrate material. Near the glass transition temperature, polymers are highly sensitive to—temperature change and strain rate. The final strain and hold time during the process significantly affect the outcome [10]. Stress relaxation is present in the process of hot embossing during the hold period after the deformation is applied as we give constant deformation and hold it for a certain period of time.

In the work done by Li et al., the pressure is increased at a rate of 0.01–0.02 MPa/s [9]. The maximum pressure to be reached is 3.2 MPa. Thus, the maximum pressure to be reached in 320–160 s (i.e., 5.3–2.6 min). The depth of the feature is 100 μm. Hence, the speed of the tool should be 0.02–0.04 mm/min.

3.1.2 Force Required. The embossing force during the process should be applied continuously so that the flow of polymer in between the mold and the substrate continues [9]. Hence, the entire PMMA substrate has to be compressed to get good quality replication.

Aluminum is chosen as the mold insert material where the features can be micromilled on the aluminum block. The dimensions of the mold insert and features are as shown in Fig. 1.

The embossing pressure is 3.2 MPa and the area of the mold insert is 736 mm^2. Hence, the force required is 2355.2 N.

Thus, we need an actuator with a load capacity of 2500 N with an accuracy of $\pm$1 N. The embossing speed is 0.02–0.04 mm/min. Therefore, an embossing speed is chosen as 0.03 mm/min with an accuracy of $\pm$0.01 mm/min.

3.1.3 Precision Requirement. The machine is developed to produce microchannels of size 100 μm with a variation of $\pm$1 μm. The parameters affecting the precision are the repeatability in locating the tool with respect to the substrate after unloading and loading of the substrate and the repeatability in the way the tool presses against the substrate.

During the embossing and de-embossing process, the mold insert should move normal to the substrate only. All other motions should be constrained in order to avoid any damage to the microfeatures.

3.2 Design Specifications. The design specifications of the setup are therefore presented in Table 1.

4 Conceptual Design of the Setup

One degree-of-freedom is required for the embossing process to replicate the features from the mold to the substrate. The overall motion of the tool is split into two linear motions—coarse and fine motion. The coarse motion helps in loading and unloading of the substrate. At the end of the coarse motion, the master mold should be properly located and aligned with respect to the substrate. The fine motion starts thereafter allowing the master mold to be pressed against the substrate. The mold and substrate pair are pressed together for the embossing time desired to ensure good replication. The mold should move normal to the substrate surface only for embossing to avoid any defect in the replication. Various concepts and methods to achieve accurate positioning and alignment, and the desired embossing motion thereafter are discussed.

4.1 Kinematic Clamp for Positioning. A kinematic clamp constrains all 6DOFs of the moving part with respect to the mating part providing precision and certainty of location [11–14]. It uses six known contact points to locate one component with respect to another. The number of contact points between any two perfectly rigid bodies is equal to the number of their mutual constraints. If a sphere is placed on a flat surface, 1DOF is constrained along the z-direction. If a sphere is placed on a v-groove, then 2DOFs are constrained as shown in Fig. 2. In a kinematic clamp, all the 6DOFs are constrained by six point contacts.

Slocum has reported that submicron repeatability can be achieved using steel ball and steel v-groove kinematic clamp [15]. Overall repeatability of the order of ten microns is reached after

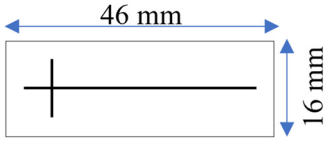

Fig. 1 Proposed mold insert

Table 1 Process parameters and specifications

Process parameters		Machine specifications		
Embossing force	2355.2 N	Force	Capacity Accuracy Resolution	2500 N ±5 N 1 N
Embossing depth	100 μm	Displacement	Range Accuracy Resolution	0–1 mm ±0.4 μm 0.1 μm
Embossing temperature	125 °C	Temperature	Range Accuracy Resolution	0 − 150 °C ±1 °C 0.1 °C
Embossing rate	(0.02–0.04) mm/min	Actuator speed	Maximum Accuracy Resolution	0.1 mm/min ±0.01 mm/min 0.01 mm/min
Other machine specifications				
Embossing capabilities	Feature size	Maximum depth Maximum area Accuracy Precision	1 mm 46 mm × 16 mm ±0.5 μm ±0.5 μm	
Material	PMMA			
Stroke	150 mm			
Machine size	600 mm × 600 mm × 1200 mm			

several hundred cycles. Hence, a kinematic clamp can be used to achieve precision in aligning the master with the substrate during the coarse motion, and thus achieving precision in the hot-embossed parts. A kinematic clamp based on three spherical balls and three radial v-grooves is proposed as shown in Fig. 3.

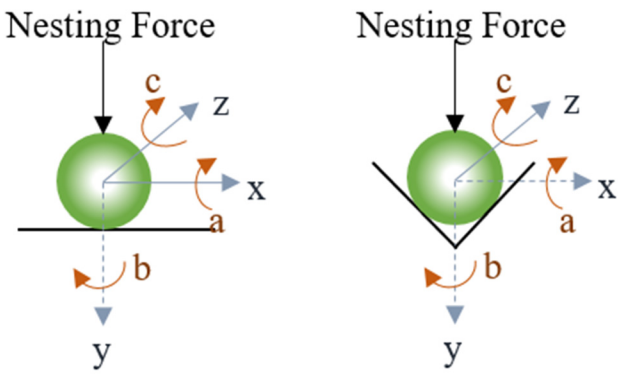

Fig. 2 (*a*) Sphere on flat surface and (*b*) sphere on a v-groove

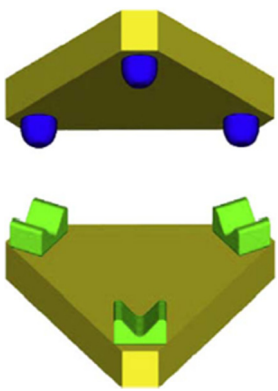

Fig. 3 Kinematic clamp based on three spherical balls and three radial v-grooves [15]

4.2 Flexures for Parallel Guidance. A flexure is a flexible element (or combination of elements) designed to be compliant in specific DOFs and to provide constraints in other directions. Flexures are used where the range of motion in the compliant direction is rather small. They provide accuracy by eliminating friction, stiction, wear, or backlash.

A sheet flexure provides constraints in 3DOFs—two translations in x- and z-directions and one rotation b about y-axis as shown in Fig. 4. A sheet flexure with a notch constrains only 2DOFs—two translations in x- and z-directions. The notch permits the rotation b about y-axis passing through the center of the two notches.

Two sheet flexures are used to achieve a parallel guidance mechanism as shown in Fig. 5. Such a mechanism can be used to achieve the up and down motion of the master mold for embossing. However, in this parallel guidance mechanism, starting at the neutral position, the body movement in x-direction is accompanied by a parasitic motion in the negative y-direction, termed as shortening effect. This is not suitable for this application. Hence, a parallel guidance mechanism with shortening compensation is proposed as shown in Fig. 6. Here, the moving body A is connected to the base through an intermediate body B via four sheet flexures on both sides.

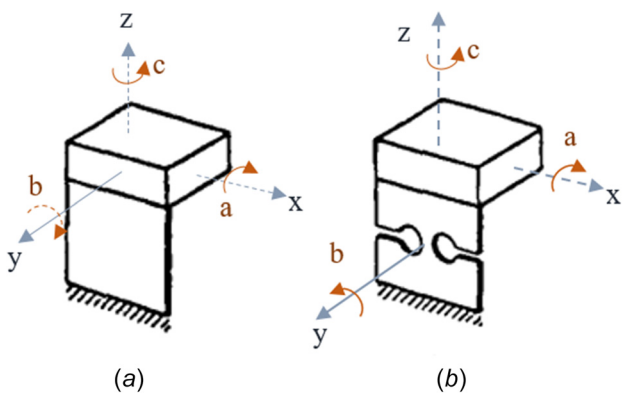

Fig. 4 (*a*) Sheet flexure and (*b*) sheet flexure with notch

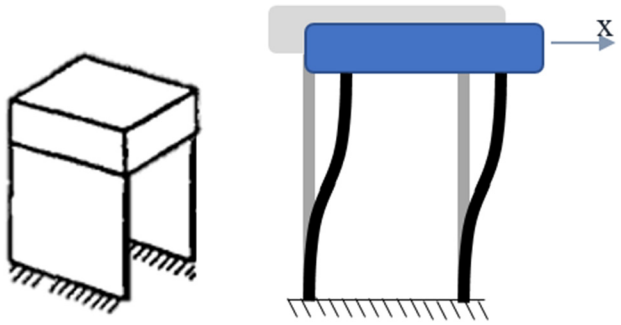

Fig. 5 Parallel guidance using flexures

4.3 Embossing Force and Heating. An embossing force needs to be applied during the embossing process. A mechanical toggle clamp with a clamping force of 386 kg is used for the development of the setup. It can be replaced by an actuator also. A thermoelectric module is used for heating the mold insert. The temperature of the insert is controlled using a pulse-width modulation (PWM)-based PID controller. An Arduino-based microcontroller is designed to control the embossing temperature.

5 Design Analysis and Computer-Aided Design Modeling

5.1 Designing of a Sheet Flexure for Parallel Guidance. The flexure in the parallel guidance mechanism can be modeled as a cantilever beam with one end fixed and the slope at the other end is zero. It is free to move in x and y-directions at the free end.

The maximum deflection is given by

$$\Delta x = \frac{\mathrm{PL}^3}{12\mathrm{EI}} \tag{1}$$

The maximum bending stress is given by

$$\sigma_{\max} = \frac{M_{\max}}{I}\frac{h}{2} \tag{2}$$

Substituting $I = bh^3/12$ and $M_{\max} = \mathrm{PL}/2$ in Eq. (2), we get

$$\sigma_{\max} = \frac{3\mathrm{PL}}{bh^2} = \frac{3Eh\Delta x}{L^2} \tag{3}$$

As shown in Fig. 7, for small movements in the negative x-direction, the shortening effect can be approximated by [14]

$$\delta = -0.6\frac{\Delta x^2}{L} \tag{4}$$

In reference to Fig. 6, let the main body A get deflected by ΔA and the intermediate body B get deflected by ΔB. Thus, the inner

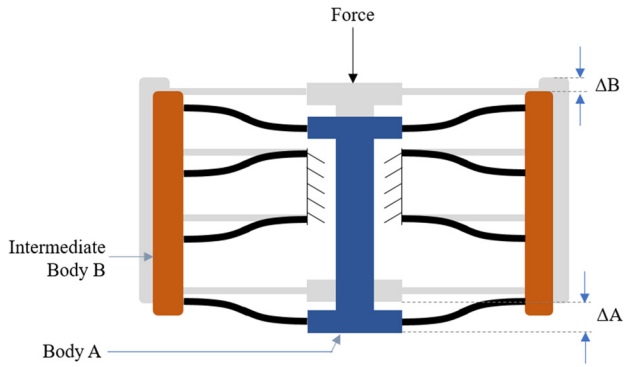

Fig. 6 Parallel guidance mechanism with shortening compensation

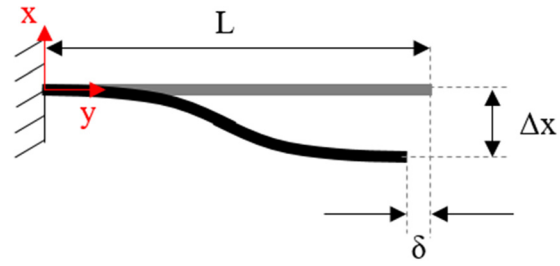

Fig. 7 Flexure in parallel guidance mechanism

set of parallel flexures get deflected by ΔB and the outer set of parallel flexures get deflected by $(\Delta A - \Delta B)$. For the shortening effect to be compensated, the shortening effect by these two sets of parallel flexures needs to be equal and in opposite directions

$$-0.6\frac{\Delta B^2}{L} = -0.6\frac{(\Delta A - \Delta B)^2}{L} \tag{5}$$

This gives $\Delta B = \Delta A/2$.

The flexures are designed for a movement of 3 mm by the body A ($\Delta A = 3$ mm). Thus, the intermediate body moves by a distance of 1.5 mm ($\Delta B = 1.5$ mm). Inner set parallel flexures each get deflected by ($\Delta B = 1.5$ mm) and outer set of parallel flexures get deflected by $(\Delta A - \Delta B) = 1.5$ mm. Hence, each flexure is to be designed for a deflection of $\Delta x = 1.5$ mm.

The dimensions of the sheet flexures used for designing the parallel guidance mechanism are shown in Fig. 8. Stainless steel 304 is selected for the fabrication of flexures. The force required for deflecting all 8 flexures to move the body A by 3 mm is 75.75 N. The deflection due to the weight of the main body (1 kg) is 0.2 mm.

5.2 Designing of Mold Insert Assembly for Thermal Expansion. The temperature of the mold insert is raised by 100 °C for the embossing process. This temperature rise will lead to thermal expansion of the insert and may give rise to thermal stresses at the joints or connections. Different concepts for the insert module were proposed and analyzed.

5.2.1 Concept 1 With Bolted Connections. In the first concept, bolted connections were used for the assembly of a mold insert, thermoelectric module, and heat exchanger as shown in Fig. 9.

Stress and deformation analysis of the insert was done using ANSYS WORKBENCH. Material properties of aluminum are used for the analysis. The von Mises stress distribution was shown in Fig. 10. The maximum stress of 757 MPa was observed near the bolted connections, which is more than the yield strength of 240 MPa of aluminum [16]. The module will fail due to thermal stresses built-up.

5.2.2 Concept 2 With Kinematic Clamp. A kinematic clamp with three pairs of spherical ball and v-groove was proposed for assembly of the module as shown in Fig. 11. In this configuration, a thermal center is defined at the point of intersection of the axis of the three v-grooves. During thermal expansion, the thermal center remains fixed and the remaining parts expand freely with respect to the center, along the grooves.

Ceramic pins with hemispherical ends were used. The insert and the top plate were kept in place using springs. During

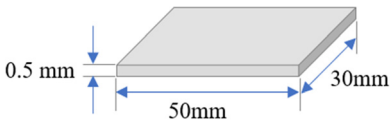

Fig. 8 Dimensions of flexure—SS 304

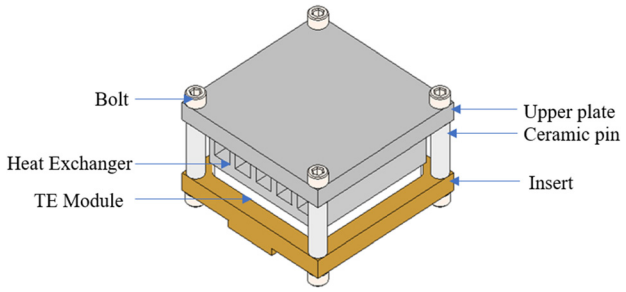

Fig. 9 Insert module with bolted connections

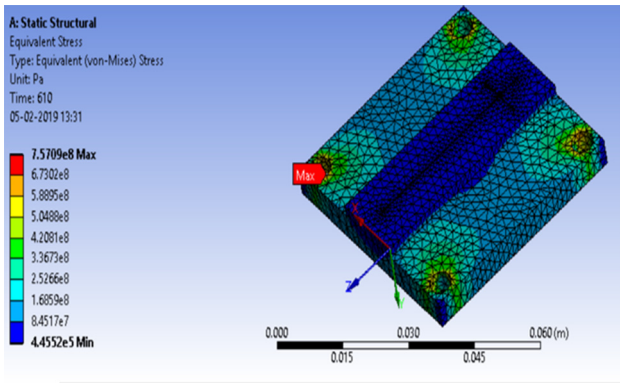

Fig. 10 von Mises stress in the insert module due to thermal load

compression, the forces get transferred through the ceramic pins. The assembly is shown in Fig. 12.

5.2.3 Concept 3 With Flexure Based Kinematic Clamp. Flexure-based kinematic clamp was proposed using three sheet

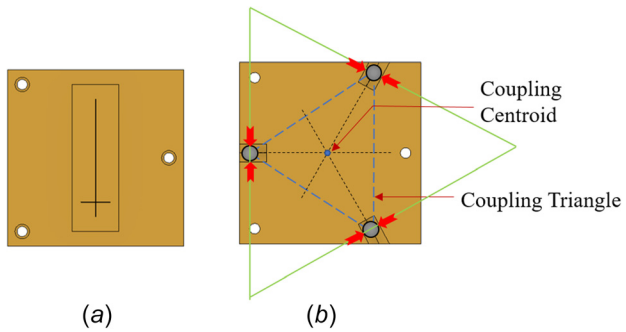

Fig. 11 (*a*) Bottom view and (*b*) top view showing coupling centroid

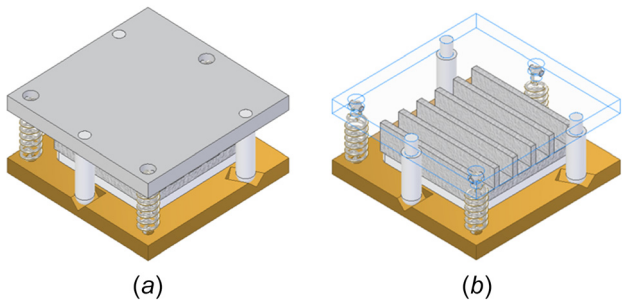

Fig. 12 (*a*) Insert assembly and (*b*) insert assembly with transparent top plate

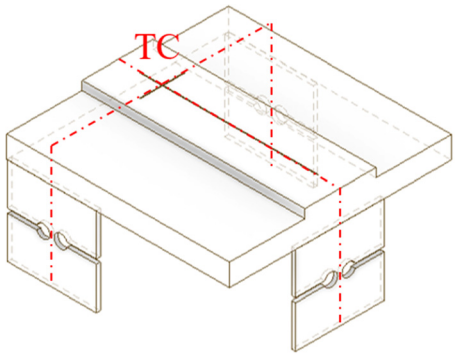

Fig. 13 6DOFs constraints with thermal center

flexures as shown in Fig. 13. The three sheet flexures with a notch provide all the six constraints. This configuration will also have the benefit of a thermal center. During the thermal expansion, the flexures allow the required internal degree-of-freedom and avoid any thermal stress build-up.

Here, the thermal center coincides with the junction of the microchannels. Thermal stresses are shown in Fig. 14. The maximum stress developed was very small. The deformation on the plate was also shown. The maximum deformation of 0.1 mm was observed at the corners.

5.3 Computer-Aided Design Modeling and Three-Dimensional Printing. A computer-aided design (CAD) model of the setup is developed as shown in Fig. 15. The setup consists of—base, toggle clamp, kinematic clamp, and insert module. A toggle clamp is attached to the base structure.

The kinematic clamp and the insert module are assembled. They are divided into upper and lower parts. The upper part includes the straight guidance mechanism and three spherical balls

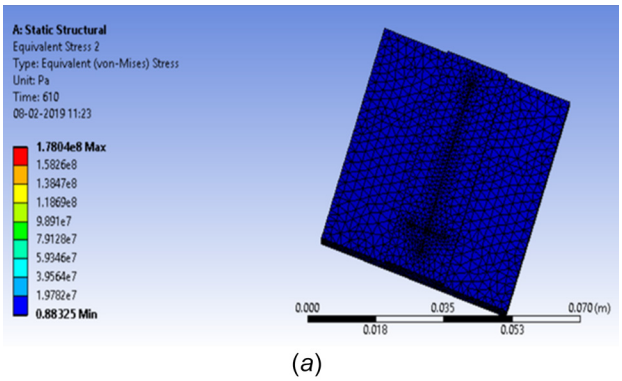

Fig. 14 (*a*) von Mises stress and (*b*) total deformation in the insert with thermal center

for clamping. The upper part rests on three radial v-grooves on the base structure through the spherical balls. CAD model of the upper part is shown in Fig. 16.

The upper part of the kinematic clamp assembly consists of a straight guidance mechanism using sheet flexures and spherical balls. Once the three spherical balls make contact with the three radial v-grooves on the base frame, the upper part gets fully constrained. The flexural straight guidance mechanism provides the fine motion required for precision hot embossing.

The lower part of the assembly includes the insert module. It has the master mold and heating element assembled together. Flexure-based kinematic clamp is used in this case. The CAD model of the insert module is shown in Fig. 17.

The upper and lower part of the assembly is placed together using T-slot features. The assembly of the insert module with the upper part of the kinematic clamp is as shown in Fig. 18.

Parts are 3D printed and assembled together. The assembly of the insert module together with the kinematic clamp is shown in Fig. 19.

6 Design of Temperature Control Module

A control module was designed to control the temperature of the insert module. Arduino-based control was developed and implemented using a thermoelectric module, heat sink, and thermocouple. Pulse width modulation based PID controller was designed and implemented.

The maximum power required for heating PMMA substrate and aluminum insert is about 100 W. A thermoelectric module, TEC1-12715, with a power rating of 250 W was chosen [17]. Aluminum heat sink was selected for heat dissipation for cooling the insert.

For temperature sensing and feedback control, Type K thermocouple was chosen with sensitivity 41 μV/°C [18]. The thermocouple was used along with a MAX6675 module [19], a thermocouple-to-digital converter with a built-in 12-bit analog-to-digital converter, and cold junction compensation.

The temperature difference between the cold and hot junction ΔT was controlled by varying the voltage (keeping the current constant) at the terminals of Peltier TEC1-12715. Pulse width modulation was used to control the average value of the voltage by varying the duty cycle.

A PID controller was designed to get a PWM signal based on the difference between the actual temperature and the desired set temperature. The required voltage to the Peltier was thus applied to achieve the required temperature at the output.

Proportional–integral–derivative control was achieved using an Arduino board which sent out a PWM signal to control the voltage to the Peltier. Since the Peltier module requires 0–15 V and 0–15 A for the required performance, a separate voltage regulator of 15 A is selected. The voltage regulator has to take the PWM signal from Arduino and should be capable of giving an output voltage that is in proportion to the PWM signal.

The block diagram of the control system is shown in Fig. 20. The complete circuit diagram was shown in Fig. 21. An LCD screen was attached for displaying the temperature measured by the thermocouple. The first stage was the heating stage where the temperature of the insert increased to embossing temperature. Once the embossing temperature was reached, the insert was clamped against the substrate using the toggle clamp. The temperature was maintained constant using a PID controller during the embossing process. After the embossing was complete, the Peltier was turned off. Once the Peltier was turned off, the insert was cooled by forced cooling using a blower fan. Once the de-embossing temperature was reached, the insert was unclamped and the substrate was removed.

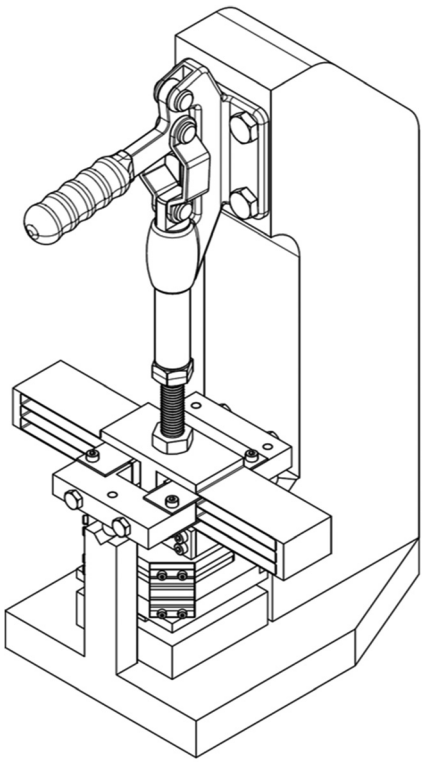

Fig. 15 CAD model of the precision hot embossing machine

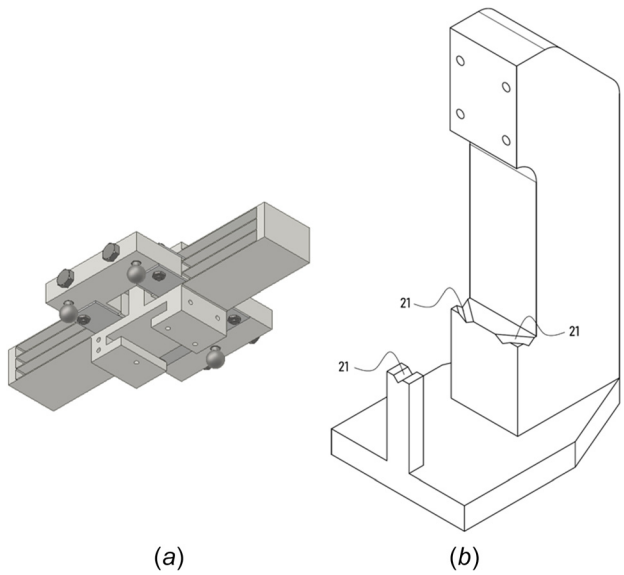

Fig. 16 (*a*) CAD model of parallel guidance mechanism with kinematic clamp, (*b*) another view showing the spherical balls, and (*c*) base structure showing three radiating v-grooves

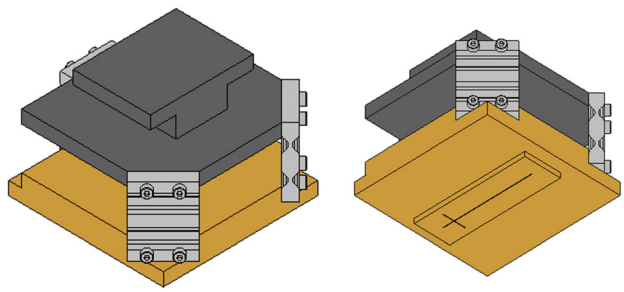

Fig. 17 Isometric views of insert module

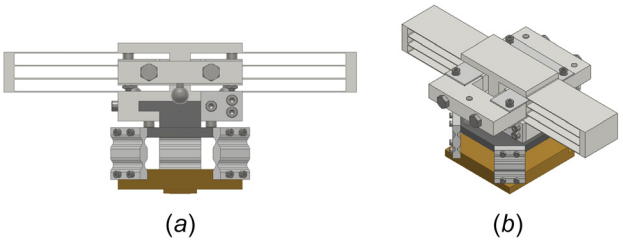

Fig. 18 (*a*) Front view and (*b*) isometric view of complete tool

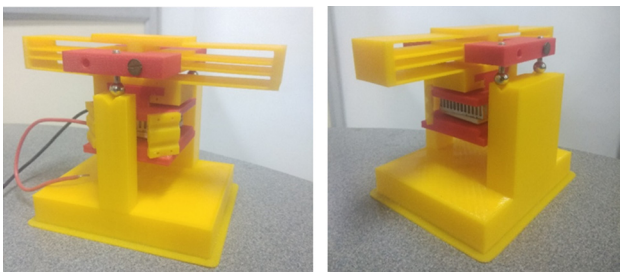

Fig. 19 3D printed assembly

6.1 Assembly of a Temperature Control Module. Insert module was assembled as shown in Fig. 22. The Peltier module was attached to an aluminum heat sink and to the insert using a thermoelectric paste. The fabricated control module was shown in Fig. 23.

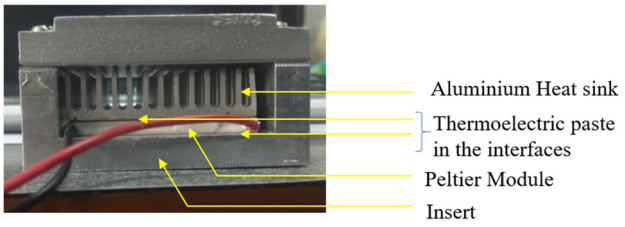

Fig. 22 Insert module with Peltier and heat sink

6.2 Design of Proportional–Integral–Derivative Controller. A PID control was designed to control the temperature of the insert. The system was assumed to be a first-order system represented as

$$G(s) = \frac{K}{\tau s + 1} \tag{6}$$

For a unit step input, the response was given by [20]

$$y(t) = K(1 - e^{-(t/\tau)}) \tag{7}$$

where K and τ were the steady-state gain and time constant.

The first-order response—the temperature of the insert—for a constant voltage input to the Peltier module was measured. For the values $K = 163$ and $\tau = 315$, the simulated first-order system response closely matched with the experimental curve as shown in Fig. 24. Here, K represented that the steady-state value of 163 °C and τ represented the time constant of 315 s to reach 63 % of the steady-state value.

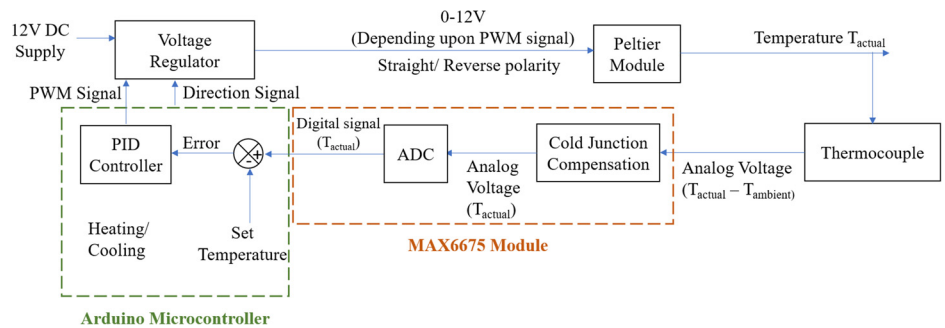

Fig. 20 Block diagram for temperature control

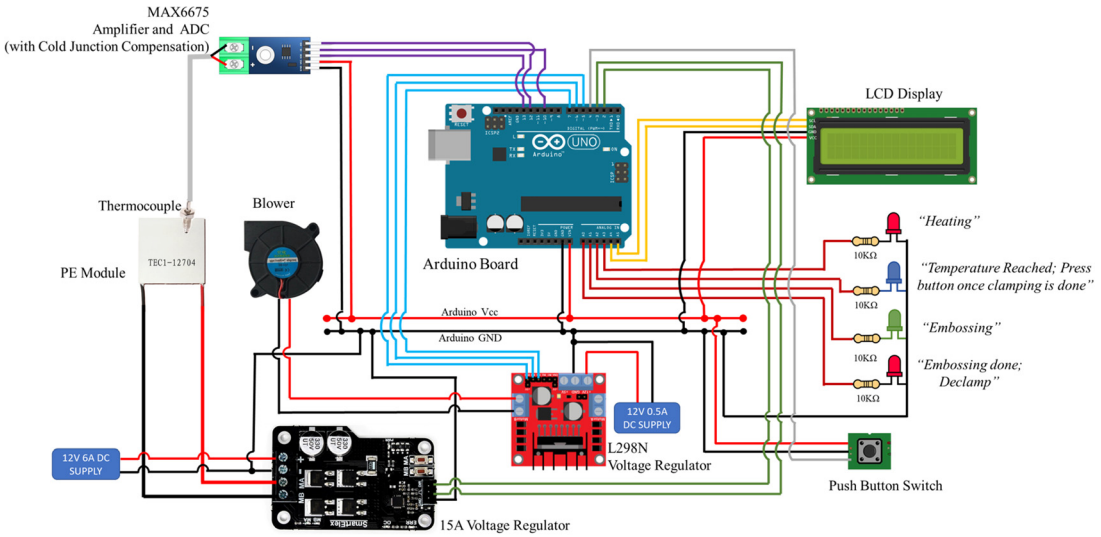

Fig. 21 Circuit diagram

The transfer function of the system thus obtained was

$$G(s) = \frac{163}{315s + 1} \tag{8}$$

A block diagram showing the proposed PID control was shown in Fig. 25. The peak temperature of 126 °C for the Peltier module was selected. The targeted embossing temperature was 125 °C. The difference was kept small to avoid damage to the Peltier module. A percentage overshoot M_p of 0.8 % and settling time of 4 min were selected for the controller design. The PID parameters thus obtained were: $K_p = 0.2$, $K_i = 0.00085$ and $K_d = 3.1909$. The step response after the PID control implementation was shown in Fig. 26.

7 Experimental Results and Discussion

An experimental setup was built using the developed insert module and control module as shown in Fig. 27. Embossing was performed on a PMMA substrate using a mechanical clamp. The insert module containing the heating unit and master was pressed against the PMMA substrate with an adequate force using the mechanical clamp.

The microfeatures on PMMA substrate were successfully embossed using a mechanical clamp and the developed

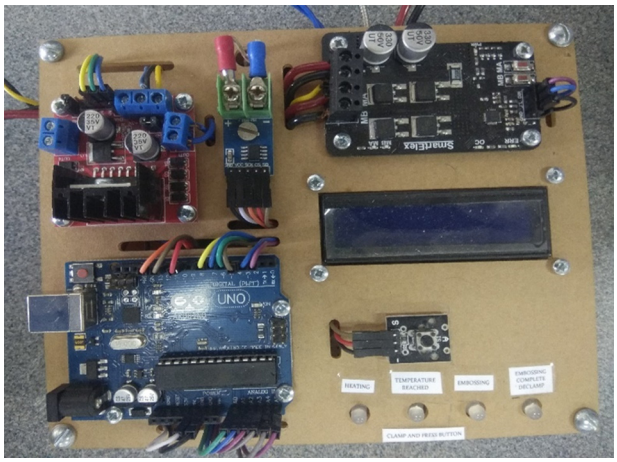

Fig. 23 Fabricated control module

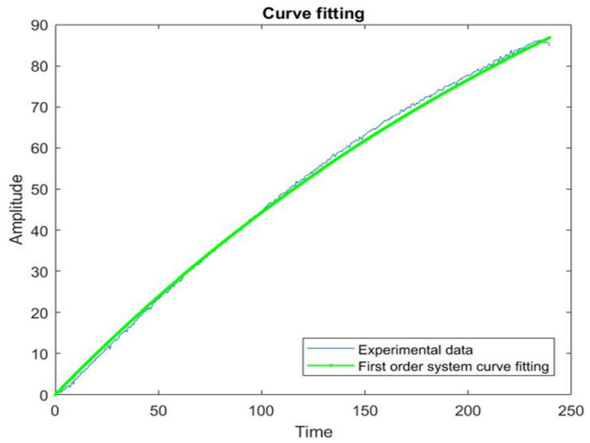

Fig. 24 Simulated first-order system response and experimental data

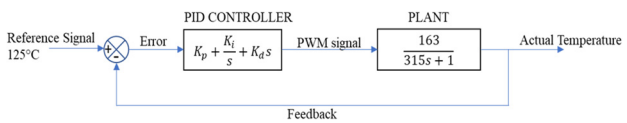

Fig. 25 Block diagram of PID controller

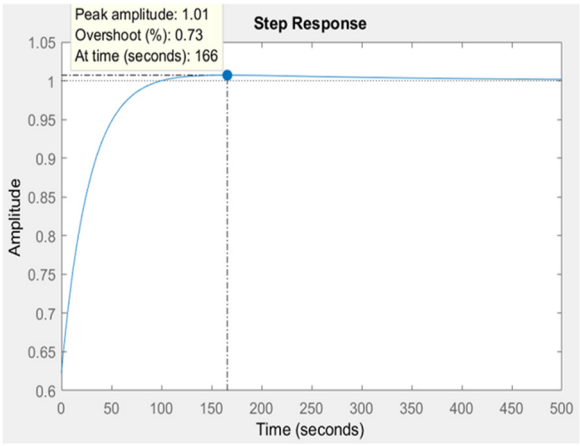

Fig. 26 Step response after implementing PID controller

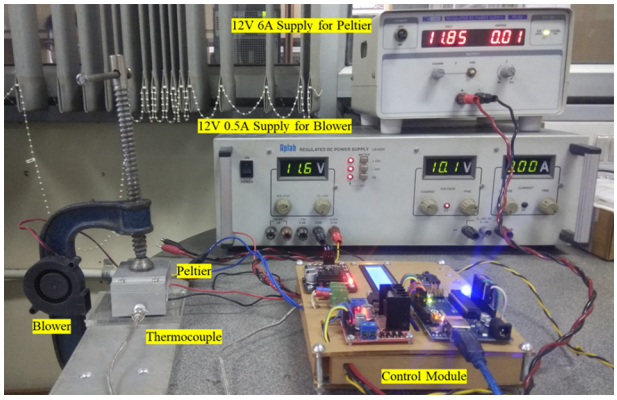

Fig. 27 Experimental setup showing developed control module and insert module. A mechanical clamp is used to provide the embossing force.

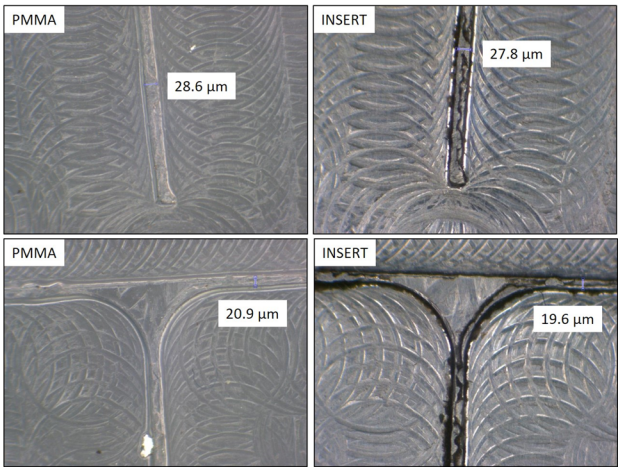

Fig. 28 Microscopic images of insert and embossed PMMA substrate

Table 2 Measurement of microfeatures on the insert and PMMA substrate

	Insert	PMMA	Deviation
Location	(μm)	(μm)	(%)
1	19.6	20.9	6.6
2	27.8	28.6	2.9

temperature control module. The microscopic images of the embossed features on the substrate were compared with the features of the mold insert as shown in Fig. 28. The measurements were taken at two locations on the insert and also at the corresponding locations on the substrate (Table 2). The microfeatures were replicated successfully from the insert to PMMA substrate. Even the tool marks on the insert were clearly visible on the substrate.

The research focuses on the design and development of the precision hot embossing machine using the principles of exact-constrained design. We eliminated the overconstraints in the assembly and applied the thermal center concept to eliminate the thermal stress build up due to heating and cooling during the embossing process. We presented the proof of concept and developed the prototype of the setup. Initial results are presented in this paper.

Dynamics of machine tools plays an important role in achieving higher precision and accuracy [21]. Huo et al. presented a holistic approach to design bench-top ultraprecision machine tools for manufacturing high-accuracy micromechanical components. A five-axis bench-top ultraprecision miromilling machine tool was developed [22,23]. The design methodology will be helpful in designing and developing our prototype and its validation. Design of machine tool structure using exact-constrained design principles helps in achieving deterministic and predictable behavior. We used 3D printed components to quickly validate our concepts. A rugged and robust prototype will be developed and investigated in detail with respect to the design specifications mentioned in Table 1 and will be presented subsequently in future.

8 Conclusion

Precision hot embossing was proposed for replicating microfluidic structures on a PMMA substrate. Kinematic design principles were used to design and develop a setup for the fabrication of these structures on the substrate. Flexure-based parallel guidance mechanism was designed for embossing action. A kinematic clamp was designed for the accurate positioning of the mold insert. The thermal module was designed and fabricated using a Peltier module. Flexure kinematic coupling with the thermal center was designed to mitigate thermal stress build-up. A temperature control module was developed and PWM-based controller was designed to control the temperature profile during the embossing process. Experiments were performed with the developed modules and microfluidic structures were embossed using the chosen process parameters. The microscopic images of the embossed features on PMMA were compared with that of the mold insert. The features were successfully replicated. The developed setup shows the efficacy of the design and the same can be used as an alternate to manufacture microfluidic chips in a cost-effective way.

Acknowledgment

The authors would like to thank Professor Sudipto Mukherjee from the Department of Mechanical Engineering, Indian Institute of Technology Delhi, India for his valuable suggestions during the design phase of the project. We would also like to acknowledge the support from the Central Research Facility, Mechatronics Lab, and Microfluidics Lab at IIT Delhi for fabrication and testing of the set-up.

References

[1] Ren, K., Zhou, J., and Wu, H., 2013, "Materials for Microfluidic Chip Fabrication," Acc. Chem. Res., **46**(11), pp. 2396–2406.
[2] Worgull, M., 2009, *Hot Embossing: Theory and Technology of Microreplication*, Elsevier, Amsterdam, The Netherlands.
[3] Çoğun, F., Yıldırım, E., and Sahir Arikan, M. A., 2017, "Investigation on Replication of Microfluidic Channels by Hot Embossing," Mater. Manuf. Process., **32**(16), pp. 1838–1844.
[4] He, Y., Wu, W., Zhang, T., and Fu, J., 2015, "Micro Structure Fabrication with a Simplified Hot Embossing Method," RSC Adv., **5**(49), pp. 39138–39144.
[5] Juang, Y.-J., Lee, L. J., and Koelling, K. W., 2002, "Hot Embossing in Microfabrication: Part I—Experimental," Polym. Eng. Sci., **42**(3), pp. 539–550.
[6] Xiaodong, W., Liding, W., Chong, L., Liqun, M., and Yi, L., 2004, "Automatic Fabrication System for Plastic Microfluidic Chips," Micro-Nanomechatronics and Human Science, and the Fourth Symposium Micro-Nanomechatronics for Information-Based Society, Nagoya, Japan, Oct. 31–Nov. 3, pp. 331–336.
[7] Lin, M.-C., Yeh, J.-P., Chen, S.-C., Chien, R.-D., and Hsu, C.-L., 2013, "Study on the Replication Accuracy of Polymer Hot Embossed Microchannels," Int. Commun. Heat Mass Transfer, **42**, pp. 55–61.
[8] Mathur, A., Roy, S., Tweedie, M., Mukhopadhyay, S., Mitra, S., and McLaughlin, J., 2009, "Characterisation of PMMA Microfluidic Channels and Devices Fabricated by Hot Embossing and Sealed by Direct Bonding," Curr. Appl. Phys., **9**(6), pp. 1199–1202.
[9] Li, J., Liu, C., and Peng, J., 2008, "Effect of Hot Embossing Process Parameters on Polymer Flow and Microchannel Accuracy Produced without Vacuum," J. Mater. Process. Technol., **207**(1–3), pp. 163–171.
[10] Brinson, H. F., and Brinson, L. C., 2008, *Polymer Engineering Science and Viscoelasticity: An Introduction*, Springer, New York.
[11] Slocum, A. H., 1992, *Precision Machine Design*, Prentice-Hall Inc., Upper Saddle River, NJ.
[12] Schellekens, P., Rosielle, N., Vermeulen, H., Vermeulen, M., Wetzels, S., and Pril, W., 1998, "Design for Precision: Current Status and Trends," Cirp Ann., **47**(2), pp. 557–586.
[13] Smith, S. T., and Chetwynd, D. G., 1992, *Foundations of Ultra-Precision Mechanism Design*, Vol. 2, Taylor & Francis Books, Singapore.
[14] Soemers, H., 2011, *Design Principles for Precision Mechanisms*, T-Pointprint, Enschede, The Netherlands.
[15] Slocum, A., 2010, "Kinematic Couplings: A Review of Design Principles and Applications," Int. J. Machine Tools Manuf., **50**(4), pp. 310–327.
[16] Beer, F., Jr., Johnston, E., DeWolf, J., and Mazurek, D., 2019, *Mechanics of Materials*, 8th ed., McGraw-Hill Education, New York.
[17] Robu.in, Macfos Pvt Ltd., 2019, TEC1-12715 40 × 40mm Thermoelectric Cooler 15A Peltier Module, accessed Jan. 2, 2019, https://robu.in/product/tec1-12715-40x40-mm-heatsink-thermoelectric-cooler-cooling-peltier-plate-module/
[18] ASTM, 1993, Manual on the Use of Thermocouples in Temperature Measurement, Fourth Ed., ASTM, West Conshohocken, PA, pp. 48–51.
[19] Robu.in, Macfos Pvt Ltd., 2019, MAX6675 Module + K Type Thermocouple Sensor Measure 1024C Temperature, accessed Jan. 2, 2019, https://robu.in/product/max6675-module-k-type-thermocouple-sensor-measure-1024-degrees-temperature/
[20] Franklin, G. F., Powell, J. D., Emami-Naeini, A., and Powell, J. D., 2002, *Feedback Control of Dynamic Systems*, Vol., 4, Prentice Hall, Upper Saddle River, NJ.
[21] Cheng, K., ed., 2009, *Machining Dynamics: Fundamentals, Applications and Practices*, Springer-Verlag, London.
[22] Huo, D., Cheng, K., and Wardle, F., 2010, "Design of a Five-Axis Ultra-Precision Micro-Milling Machine–Ultramill: Part 1—Holistic Design Approach, Design Considerations and Specifications," Int. J. Adv. Manuf. Technol., **47**(9–12), pp. 867–877.
[23] Huo, D., Cheng, K., and Wardle, F., 2010, "Design of a Five-Axis Ultra-Precision Micro-Milling Machine–Ultramill: Part 1—Holistic Design Approach, Design Considerations and Specifications," Int. J. Adv. Manuf. Technol., **47**(9–12), pp. 879–890.